

Theoretical Studies on the Structures and Stabilities of Charged, Titanium-Doped, Small Silicon Clusters, $\text{TiSi}_n^-/\text{TiSi}_n^+$ ($n = 1-8$)

Chengzhi Deng · Liqing Zhou · Guoliang Li ·
Hongyu Chen · Qian-shu Li


Received: 2 December 2011
© Springer Science+Business Media, LLC 2012

Abstract The structures and stabilities of charged, titanium-doped, small silicon clusters $\text{TiSi}_n^+/\text{TiSi}_n^-$ ($n = 1-8$) have been systematically investigated using the density functional theory method at the B3LYP/6-311+G* level. For comparison, the geometries of neutral TiSi_n clusters were also optimized at the same level, although most of them have been reported previously (Guo et al., J Chem Phys 126: 234704, 2007). Our results indicate that all neutral TiSi_n clusters favor Si-capped TiSi_{n-1} structures, with the lowest energy structure of TiSi_2 , TiSi_3 , TiSi_4 , TiSi_5 , TiSi_6 , TiSi_7 and TiSi_8 being Si-side-on TiSi adduct, Si-face-capped TiSi_2 triangle, Si-face-capped TiSi_3 trigonal pyramid, Si-face-capped TiSi_4 trigonal bipyramid, Si-face-capped TiSi_5 square bipyramid, Si-face-capped TiSi_6 pentagonal bipyramid, and Si-face-capped TiSi_7 capped pentagonal bipyramid, respectively. The ground state structures obtained herein for the neutral TiSi_n clusters agree well with those of Guo et al. except for TiSi_3 and TiSi_8 . Adding or removing an electron greatly changes some ground state structures, i.e. for $\text{TiSi}_3^-/\text{TiSi}_3^+$, TiSi_5^- , $\text{TiSi}_6^-/\text{TiSi}_6^+$, TiSi_7^- and $\text{TiSi}_8^-/\text{TiSi}_8^+$; others are almost unchanged, e.g. $\text{TiSi}_2^-/\text{TiSi}_2^+$, $\text{TiSi}_4^-/\text{TiSi}_4^+$, TiSi_5^+ and TiSi_7^+ . Based on the optimized geometries, various energetic properties, including binding energies, fragmentation energies, second-order difference energies, HOMO–LUMO energy gaps, ionization potentials and electron affinities, were calculated for all the most stable isomers. The average binding energies reveal that all of $\text{TiSi}_n/\text{TiSi}_n^+/\text{TiSi}_n^-$ ($n = 1-8$) clusters can continue to gain energy as the size increasing. The fragmentation energies and second-order energy

C. Deng · L. Zhou · G. Li (✉) · H. Chen (✉) · Q. Li
MOE Key Laboratory of Theoretical Chemistry of the Environment, School of Chemistry and
Environment, South China Normal University, Guangzhou 510006, Guangdong,
People's Republic of China
e-mail: glli@sncu.edu.cn

H. Chen
e-mail: hychen@sncu.edu.cn

Published online: 10 May 2012

 Springer

differences suggest that neutral TiSi_5 , anionic TiSi_5^- and cationic TiSi_6^+ are relatively stable.

Keywords Titanium-doped silicon clusters · Structures · Stabilities · Density functional theory

Introduction

Silicon clusters form a link between isolated silicon atoms and bulk silicon materials, and have attracted extensive interests in the past decades. Experimentally, Cheshnovsky et al. [1] measured the ultraviolet photoelectron spectra of the Si_n^- ($n = 3\text{--}12$) anions in 1987, yielding electron affinities and qualitative pictures of the electronic states for neutral Si_n clusters. Neumark et al. [2–6] measured photoelectron spectra of the Si_n^- ($n = 2\text{--}7$) clusters at several photodetachment energies in 1990s, obtaining the electronic states, electron affinities, term energies and vibrational frequencies for the ground and excited electronic states of neutral Si_n clusters. Theoretically, Raghavachari et al. [7–18] have investigated the structures, stability, and electronic properties of $\text{Si}_n/\text{Si}_n^-$ ($n \leq 11$) using ab initio methods in 1980s and 1990s. Fournier et al. [19] have studied the properties of Si_n ($n = 2\text{--}8$) using density functional theory (DFT) method in 1992.

Although silicon and carbon are in same group in periodic table, they have many different properties. Carbon prefers sp or sp^2 hybridization to form linear or fullerene-like cage structures [20], but silicon prefers sp^3 hybridization when clustering, which makes pure silicon clusters are highly reactive due to surface dangling bonds [21–23]. Numerous works have reported the formation of transition metal (TM)-doped silicon clusters, finding that TM atoms can saturate the dangling bond of the silicon clusters and thus stabilize the silicon clusters. As early as the late 1980s, Beck [24, 25] initially produced mixed TMSi_n (TM = Cr, Mo, W, Cu) clusters in a supersonic molecular beam. But the study of TM-doped silicon clusters started thriving only until 2001 when Hiura et al. [26] examined the stable cage-like $\text{TM}@\text{Si}_n^+$ (TM = Hf, Ta, W, Re, Ir, etc.; $n = 14, 13, 12, 11, 9$) clusters combining experimental and theoretical methods. Then, many researchers joined the quest for a deeper understanding of TM-doped silicon clusters, and the ScSi_n ($n = 1\text{--}6$) [27], ScSi_n^- ($n = 2\text{--}6$) [28], TiSi_n ($n = 2\text{--}15$) [29], VSi_n^- ($n = 3\text{--}6$) [30], CrSi_n ($n = 1\text{--}6, 8\text{--}17$) [31, 32], CrSi_n^- ($n = 8\text{--}12$) [33], MnSi_n ($n = 1\text{--}15$) [34], FeSi_n ($n = 2\text{--}14$) [35, 36], CoSi_n ($n = 2\text{--}14$) [37], NiSi_n ($n = 1\text{--}17$) [38–40], CuSi_n ($n = 4, 6, 8\text{--}14$) [41, 42], YSi_n ($n = 1\text{--}16$) [43], ZrSi_n ($n = 1\text{--}16$) [44], MoSi_n ($n = 1\text{--}6$) [45], AgSi_n ($n = 1\text{--}13$) [46], TaSi_n ($n = 1\text{--}13$) [47], TaSi_n^+ ($n = 1\text{--}13$, and 16) [48], WSi_n ($n = 1\text{--}6$, and 12) [49], ReSi_n ($n = 1\text{--}12$) [50], IrSi_n ($n = 1\text{--}6$) [51], and AuSi_n ($n = 1\text{--}16$) [52] clusters were systematically investigated. Most recently, combining infrared multiple photon dissociation spectroscopy and DFT methods, Ngan et al. [53] described the growth mechanisms of small cationic silicon clusters exohedrally doped by V and Cu atoms (MSi_n^+ , $n = 4\text{--}11$ for V, and $n = 6\text{--}11$ for Cu), finding that V prefers substitution of a silicon atom in a highly coordinated position of the cationic bare silicon clusters while Cu favors adsorption to the

neutral or cationic bare clusters in a lower coordination site. They also investigated the VSi_n^+ ($n = 12\text{--}16$) clusters, showing that these clusters have endohedral caged structures and, especially, VSi_{16}^+ is a fluxional system with a symmetric Frank–Kasper geometry [54].

As a TM, titanium is extensively studied as a candidate of doping atoms. Titanium silicides have been widely used in ultra-large-scale integration technologies due to relative low resistivity ($10\text{--}28\ \mu\Omega\ \text{cm}$), high thermal stability, and low work function [55–57]. Ohara et al. [58] studied geometric and electronic structures of TM-doped silicon clusters (TM = Ti, Hf, Mo and W) by the use of mass spectrometry, chemical-probe method and photoelectron spectrometry in 2003, finding that their electron affinities have a minimum at $n = 16$. Two years latter, Koyasu et al. [59] studied the electronic and geometric structures of mixed metal silicon clusters TMSi_{16} (TM = Sc, Ti, and V) using mass spectrometry and anion photoelectron spectroscopy, finding that neutral TiSi_{16} has closed-shell electron configuration with a large energy gap between the highest occupied molecular orbital (HOMO) and the lowest unoccupied molecular orbital (LUMO). Several theoretical studies were also performed on Ti-doped silicon clusters. In 2003, Sen et al. [60] reported the electronic structures of Ti-encapsulated Si_{12} hexagonal prism cage, and found that for TiSi_{12} the triplet state has lower energy and Ti d electrons do not form strong covalent bonds with Si_{12} cage. In the next year, Kawamura et al. [61] investigated the adsorption of H_2O molecules on Ti-doped silicon clusters and found that TiSi_n clusters form a cage structure from $n = 13$ onwards so that H_2O adsorption could occur only up to $n = 12$. Kawamura et al. [62] also studied the growth behavior of TM-doped silicon clusters (TM = Ti, Zr, Hf; $n = 8\text{--}16$) in 2005, and the results indicated that TiSi_n clusters form basket structures up to $n = 12$ and cage structures from $n = 13$ onwards. Guo et al. [29] investigated the geometries, stabilities, and electronic properties of TiSi_n ($n = 2\text{--}15$) clusters by using density-functional theory approach at the B3LYP/LanL2DZ level, and found that the equilibrium site of the Ti atom gradually moves from convex to surface and then to a concave site as the number of the Si atoms increases from 2 to 15. The Ti atom in TiSi_{12} completely falls into the center of the Si outer frame, forming metal-encapsulated Si cages. Recently, Reis et al. [63] investigated the feasibility of assembling the exceptionally stable isovalent XSi_{16} ($\text{X} = \text{Ti, Zr and Hf}$) nanoparticles to form new bulk materials employing the first-principles DFT, and the results suggest that new pathways through which endohedral cage clusters may constitute a viable means toward the production of synthetic materials with pre-defined physical and chemical properties.

Many of the works mentioned above on the TiSi_n clusters are for slightly larger ($n > 8$) clusters while the studies on small size ($n < 8$) clusters are far from systematic. Furthermore, charged $\text{TiSi}_n^{+/-}$ clusters have never been investigated to date to our knowledge, though the experimental observations were usually based on mass spectrometric measurements in which charged clusters were produced. Therefore, more theoretical researches on charged $\text{TiSi}_n^{+/-}$ clusters are still necessary. In this paper, we carried out a detailed investigation on the structures, stabilities, and the growth pattern of neutral and charged Ti-doped small silicon clusters $\text{TiSi}_n^-/\text{TiSi}_n^+/\text{TiSi}_n^0$ ($n = 1\text{--}8$). The computational details are described in

“Computational Methods” section while the results and discussion are shown in “Result and Discussion” section.

Computational Methods

All calculations were carried out with Gaussian 03 program package [64]. Briefly, the clusters were examined using DFT method at the B3LYP/6-311+G* level of theory. The B3LYP represents a hybrid Hartree–Fock (HF)/DFT method using a combination of Becke’s three-parameter exchange functional (B3) [65] with the Lee–Yang–Parr (LYP) [66] generalized gradient correlation functional. The 6-311G specifies the McLean–Chandler (12s9p)/[6s5p] basis set for the Si atoms [67, 68] and the Wachters–Hay all electron basis set [69, 70], utilizing the scaling factors of Raghavachari and Trucks [71], for the Ti atom. Since the inclusion of both cations and anions in this study, the 6-311G basis sets were augmented with *d*-polarization functions and diffuse *sp*-functions. As known, the DFT-B3LYP/6-311+G* method has been successfully applied to researches of many heteroatom-doped silicon clusters [27, 30, 41]. Harmonic vibrational frequencies were computed at the same computational level to estimate the nature of the stationary points. The default integration grid (pruned 75,302) of Gaussian 03 was mainly applied for evaluating integrals numerically, but we also employed the finer grid (99,590) to check some suspicious results when necessary.

Result and Discussion

To find the lowest-energy isomers, various initial structures of $\text{TiSi}_n/\text{TiSi}_n^-/\text{TiSi}_n^+$ were constructed mainly by following ways: (1) placing a Ti atom at various attaching sites of the Si_n structures; (2) substituting a Ti atom for one of the Si atoms in the Si_{n+1} structures; (3) placing a Si atom at various attaching sites of the TiSi_{n-1} structures; (4) considering all possible structures of other impurity-doped Si clusters reported in previous papers, etc. For each structure, three electronic states with different multiplicities, i.e. the singlet, triplet and quintet states for neutral TiSi_n , plus the doublet, quartet and sextet states for ionic $\text{TiSi}_n^-/\text{TiSi}_n^+$, were considered. However, only the lower-energy structures (with their relative energies within ~ 15 kcal/mol), as illustrated in Figs. 1 and 2, are discussed in this article.

Geometries and Stabilities

Comparing with the B3LYP/LanL2dZ results of Guo et al. [29] for TiSi_n , we got similar low-lying structures for $n \leq 6$ but in a different energetic order for some clusters. For $n = 7-8$, our results did not agree with theirs. Thus the neutral Ti-doped silicon clusters would still be mentioned in later discussion along with the anionic and cationic clusters.

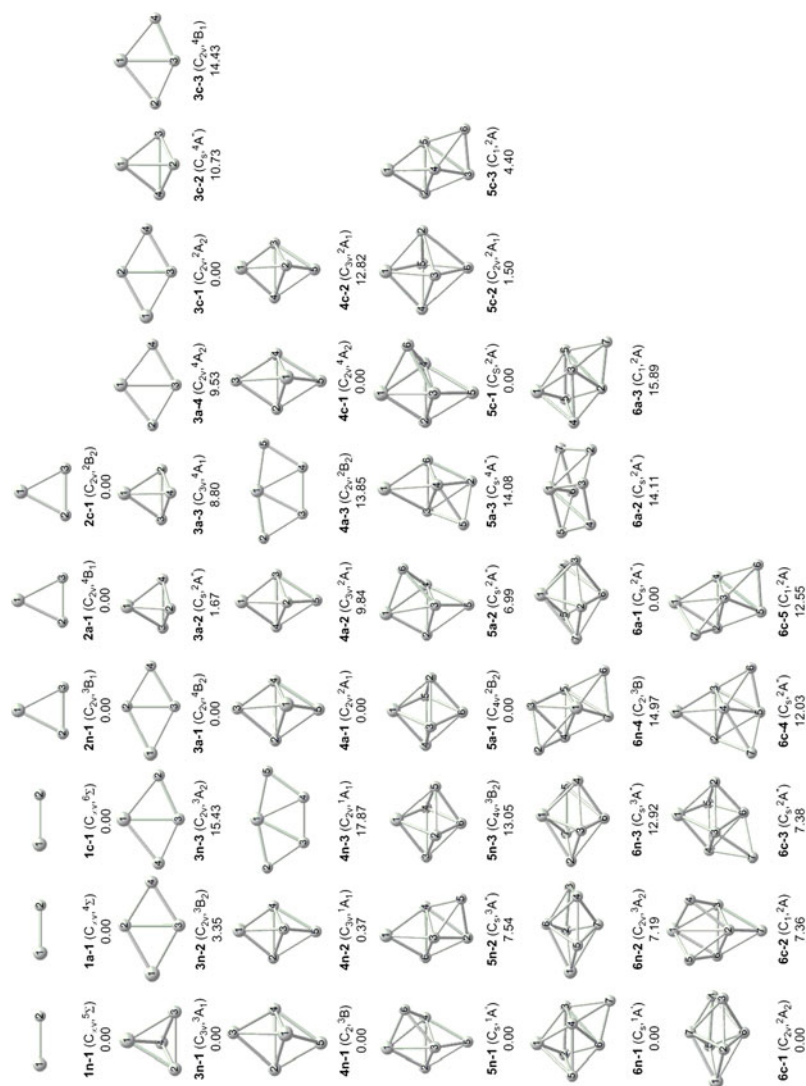


Fig. 1 The low-energy structures of $\text{TiSi}_n^-/\text{TiSi}_n^+$ ($n = 1-6$) clusters. The Ti atom is marked "1". The electronic state, symmetry, and energy difference (in kcal/mol) relative to the ground state are given below the structure for each size. For the **ix-j** notation: **i** is the number of silicon atoms, n ; **x** = **n** for neutral, **a** for anionic, **c** for cationic; **j** = **1** for the ground state, **2** for the next lowest energy, etc

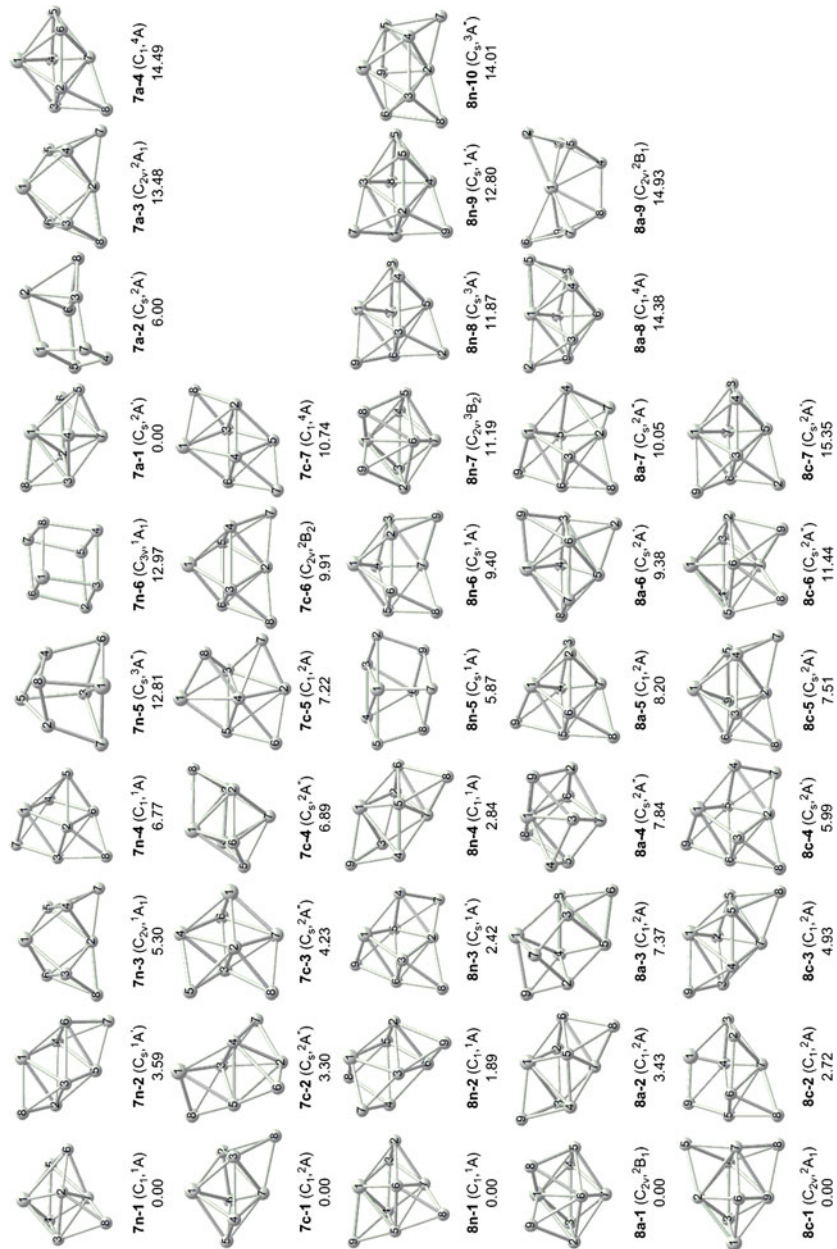


Fig. 2 The low-energy structures of $\text{TiSi}_n/\text{TiSi}_n^+$ ($n = 7-8$) clusters. The Ti atom is marked "I"

$n = 1$

For neutral TiSi , the predicted lowest energy isomer (**1n-1**) is in spin quintet, as shown in Fig. 1, different from ZrSi [44] which has a spin singlet configuration as most stable. For ionic TiSi^- and TiSi^+ , the lowest lying isomer is in spin quartet (**1a-1**) and sextet state (**1c-1**), respectively. For each cluster, the calculated bond lengths show a dependence on spin state as being elongated when spin state changing from low to high. The Ti–Si bond lengths of **1n-1**, **1a-1** and **1c-1** are 2.449, 2.371 and 2.451 Å, respectively, i.e. the anion has a shorter Ti–Si bond than the neutral while the cation has a longer bond. This could be related with their electronic configurations: $\dots 10\sigma^2 4\pi^2 1\delta 11\sigma$ for **1n-1**, $\dots 10\sigma^2 4\pi^3 1\delta 11\sigma$ for **1a-1**, $\dots 10\sigma 4\pi^2 1\delta 11\sigma$ for **1c-1**, respectively. Adding an electron strengthens the Ti–Si bond; while taking away an electron weakens it.

$n = 2$

The lowest energy structure of neutral TiSi_2 is a C_{2v} isosceles triangle with $^3\text{B}_1$ electronic state (**2n-1**), same with the result of Guo et al. [29]. The Ti–Si and Si–Si bond lengths in **2n-1** are 2.411 and 2.225 Å, respectively. The energies of corresponding singlet and quintet states are higher than **2n-1** by 16.69 and 22.31 kcal/mol, respectively. Two possible linear structures of TiSi_2 are found extremely high in energy or having imaginary frequencies, and previous work [40] also found linear structures for TMSi_2 clusters remarkably high in energy.

Ionic TiSi_2^- and TiSi_2^+ also have their ground state structures being isosceles triangle, **2a-1** and **2c-1** as shown in Fig. 1. The Ti–Si and Si–Si bond lengths in the former are 2.504 Å and 2.201 Å, in the latter are 2.419 and 2.245 Å. Thus, adding an electron to the TiSi_2 cluster compresses the triangle whereas removing an electron expands the triangle, indicating that the interaction between the two Si atoms is strengthened as the number of electrons increases. The electronic states of **2a-1** and **2c-1** are $^4\text{B}_1$ and $^2\text{B}_2$, respectively.

The lowest lying linear Ti–Si–Si structure of TiSi_2^- is with $^4\Sigma$ state and higher in energy than **2a-1** by 30.78 kcal/mol. The identical linear structure of TiSi_2^+ reaches minimum when in $^2\Sigma$ state and is 18.64 kcal/mol above **2c-1**.

We can not find stable linear Si–Ti–Si structures for either TiSi_2^- or TiSi_2^+ . The optimization results have imaginary frequencies and the normal modes of imaginary frequencies leading to triangle structures.

$n = 3$

For TiSi_3 , the predicted global minimum has a geometry of C_{3v} trigonal pyramid (**3n-1**). It is different from the result of Guo et al. [29] which shows a rhombus similar to our **3n-2** isomer (vide infra) as the lowest energy structure. Comparatively, ZrSi_3 [44] also has a trigonal pyramid as the ground state structure. The electronic state of **3n-1** is $^3\text{A}_1$.

The low-lying structure **3n-2** is a C_{2v} deformed rhombus with $^3\text{B}_2$ state, which can be seen as a Si atom capping on the Si–Si edge of the TiSi_2 isomer **2n-1**.

Structure **3n-2** is 3.35 kcal/mol higher in energy than **3n-1**. Another rhombic structure **3n-3** with 3A_2 state is energetically 15.43 kcal/mol above **3n-1**. It is different from **3n-2** in that the Si atom caps on the Ti–Si edge of **2n-1**.

The ground state structure of both $TiSi_3^-$ (**3a-1**) and $TiSi_3^+$ (**3c-1**) is C_{2v} planar rhombus, similar to the low-lying neutral structure **3n-2**. The electronic states of **3a-1** and **3c-1** are 4B_2 and 2A_2 , respectively. The Ti–Si bond length, Si₂–Si₄ bond length and the angle of Si₂–Ti₁–Si₃ are 2.593, 2.309 Å and 54.0° for **3a-1**, and 2.420, 2.354 Å and 57.7° for **3c-1**.

The second low-lying structure of $TiSi_3^-$ (**3a-2**) and $TiSi_3^+$ (**3c-2**) is C_s trigonal pyramid with the Ti atom at the apex, higher in energy than the corresponding ground state by 1.67 and 10.73 kcal/mol respectively. It can be seen as a Si atom face-capped on the ground state structure of $TiSi_2^-$ (**2a-1**) or $TiSi_2^+$ (**2c-1**). Another trigonal pyramid structure (**3a-3**) of $TiSi_3^-$ with C_{3v} symmetry and 4A_1 state lies energetically 8.80 kcal/mol above the ground state **3a-1**.

There is another rhombus structure for anionic $TiSi_3^-$ (**3a-4**) and cationic $TiSi_3^+$ (**3c-3**) with the Ti atom on the obtuse angle vertex. Structure **3a-4** with 4A_2 state and **3c-3** with 4B_1 state lie energetically above corresponding ground state (**3a-1** and **3c-1**) by 9.53 and 14.43 kcal/mol, respectively. The angle of Ti₁–Si₂–Si₃ in **3a-4** and **3c-3** is 68.6° and 63.4°, respectively.

Comparing the low-lying isomers of ionic $TiSi_3^-/TiSi_3^+$ with those of neutral $TiSi_3$ finds that the addition/removal of an electron to/from the neutral cluster changes the relative order of isomer stability, and results in the transformation of the lowest-energy structure from a more compact tridimensional trigonal pyramid to the plane rhombus structure.

$n = 4$

The ground state of neutral $TiSi_4$ cluster (**4n-1**) has a trigonal bipyramid structure with the Ti atom on an equatorial position, having C_2 symmetry and in 3B state, which is lower in symmetry than the C_{2v} pyramid structure gained by Guo et al. [29]. Our ground state structure of $TiSi_4$ is in agreement with that of $ScSi_4$ [27]. Structure **4n-1** can be viewed as a Si atom capping on the Ti–Si–Si face of $TiSi_3$ (**3n-1**). Another low-lying structure **4n-2** is a C_{3v} trigonal bipyramid with the Ti atom on the axial position, which is only 0.37 kcal/mol higher in energy than **4n-1**. Structure **4n-2** can be seen as a Si atom capping on the bottom of $TiSi_3$ (**3n-1**).

Adding or removing an electron does not change the stereochemistry of the $TiSi_4$ cluster, even the relative order of isomer stability. Thus, the ground states of $TiSi_4^-$ and $TiSi_4^+$ have structures similar to **4n-1**, with 2A_1 state for $TiSi_4^-$ (**4a-1**) and 4A_2 for $TiSi_4^+$ (**4c-1**), both of them have C_{2v} symmetry. Among the low-lying structures, **4a-2** of $TiSi_4^-$ and **4c-2** of $TiSi_4^+$ are similar to **4n-2**, higher in energy than corresponding **4a-1** and **4c-1** by 9.84 and 12.82 kcal/mol, respectively. Another $TiSi_4^-$ isomer **4a-3**, with a C_{2v} planar pentagon structure shaped like a trapezoid, lying energetically above ground state by 13.85 kcal/mol. Besides, structure **4a-3** can be seen as a Si atom capping on the Ti–Si edge of $TiSi_3^-$ isomer **3a-4**.

$n = 5$

The ground state we obtained for TiSi_5 (**5n-1**) has similar geometry with that of Guo et al. [29], which can be viewed as a Si atom capping on the Ti–Si–Si face of low-lying TiSi_4 structure **4n-2**. Previous works for ZrSi_5 [44] and ScSi_5 [27] also showed a face-capped trigonal bipyramid to be the lowest energy structure. Structure **5n-1** has C_s symmetry and singlet $^1A'$ state, different from Guo et al.'s result which indicating a C_1 symmetry. Isomer **5n-2** also has a face-capped trigonal bipyramid structure, but with a Si atom capping on the Si–Si–Si face, which is energetically higher than the ground state **5n-1** by 7.54 kcal/mol. Another low-lying structure **5n-3** is a tetragonal bipyramid with the Ti atom on an apex. Structure **5n-3** has C_{4v} symmetry and is higher in energy than the ground state **5n-1** by 13.05 kcal/mol.

Similar to TiSi_3 , the addition/removal of an electron changes the relative order of the TiSi_5 isomer stability, though the above mentioned three structures for neutral TiSi_5 are also found for low-lying isomers of anionic TiSi_5^- and cationic TiSi_5^+ clusters. The lowest energy isomer **5a-1** of TiSi_5^- has a C_{4v} square bipyramid structure similar to **5n-3**. The electronic state is 2B_2 . The axial-equatorial Ti–Si bond length in **5a-1** is 2.480 Å, the axial-equatorial Si–Si bond length is 2.471 Å, and equatorial Si–Si bond length is 2.572 Å. Isomers **5a-2** and **5a-3**, with geometry similar to **5n-1** and **5n-2** respectively, lie energetically higher than **5a-1** by 6.99 and 14.08 kcal/mol, respectively. The electronic states are $^2A''$ for **5a-2** and $^4A''$ for **5a-3**.

The ground state structure of TiSi_5^+ (**5c-1**) is a trigonal bipyramid with a Si atom capping on a Ti–Si–Si face, which is analogous to **5n-1**. Isomer **5c-2** has a square bipyramid structure with C_{2v} symmetry and 2A_1 state, being higher in energy than **5c-1** by only 1.50 kcal/mol. Another isomer **5c-3**, with **5n-2** like structure, a Si–Si–Si face-capped trigonal bipyramid, is 4.40 kcal/mol higher in energy than **5c-1**.

$n = 6$

Isomer **6n-1** is predicted to be the ground state of neutral TiSi_6 cluster, which can be seen as a Si atom capping on a Si–Si–Si face of the TiSi_5 structure **5n-3**, in agreement with Guo et al.'s result [29]. Similar structure is also found as the ground state structure of ZrSi_6 [44]. Structure **6n-1** has C_s symmetry and $^1A'$ electronic state. Next two low-lying structures of TiSi_6 are pentagonal bipyramid, one with the Ti atom on an equatorial vertex (**6n-2**) and the other with the Ti atom on an apex (**6n-3**). They are energetically higher than **6n-1** by 7.19 and 12.92 kcal/mol, respectively. The symmetry and electronic state are C_{2v} and 3A_2 for **6n-2** while C_s and $^3A''$ for **6n-3**. Another structure **6n-4** is a bicapped trigonal bipyramid with the Ti atom on an equatorial vertex and two Si atoms capping on two Ti–Si–Si faces. With C_2 symmetry and 3B state, structure **6n-4** lies higher in energy than **6n-1** by 14.97 kcal/mol.

The ground state of TiSi_6^- (**6a-1**) has a pentagonal bipyramid structure similar to **6n-3**. The electronic state is $^2A''$. Isomer **6a-2** with a Ti-face-capped chair-like

structure lies above **6a-1** by 14.11 kcal/mol. Another isomer **6a-3** has a face-capped square bipyramid structure like **6n-1** and is 15.89 kcal/mol higher in energy than the ground state **6a-1**.

The lowest energy structure of TiSi_6^+ (**6c-1**) is also a pentagonal bipyramid with the Ti atom on an equatorial vertex, like **6a-1**. It displays C_{2v} symmetry and 2A_2 electronic state. Structure **6c-2** is a trigonal bipyramid with two Ti–Si–Si faces capped by two more Si atoms. Isomers **6c-4** and **6c-5** also have geometry of bicapped trigonal bipyramid, though there are two Si-capped Si–Si–Si faces in the former but one Si-capped Ti–Si–Si face and one Si-capped Si–Si–Si face in the latter. Structures **6c-2**, **6c-4** and **6c-5** lie above ground state by 7.36, 12.03 and 12.55 kcal/mol, respectively. Isomer **6c-3** has a capped square bipyramid structure like neutral **6n-1**. It is energetically 7.38 kcal/mol above the ground state of **6c-1**.

$n = 7$

Structure **7n-1** is predicted to be the ground state of neutral TiSi_7 . It is an irregular capped pentagonal bipyramid structure (C_1) with the Ti atom on the apex and one Si atom capping on a Si–Si–Si face, which does not agree with Guo et al.'s result [29]. Isomer **7n-1** displays a singlet 1A electronic state. Structures **7n-2** and **7n-4** can be viewed as adding a Ti–Si–Si face-capping Si atom on the capped square bipyramid structure **6n-1** while structure **7n-3** adding a Si–Si–Si face-capping Si atom on **6n-1**. Isomer **7n-2**, **7n-3**, and **7n-4** are 3.59, 5.30 and 6.77 kcal/mol higher in energy than **7n-1**. Structures **7n-5** and **7n-6** can be seen as distorted cubes. **7n-5** is more twisted than **7n-6** and is energetically 12.81 kcal/mol above the ground state **7n-1**. **7n-6** has C_{3v} symmetry and is 12.97 kcal/mol higher than the ground state **7n-1**.

The ground state of anionic TiSi_7^- cluster (**7a-1**) displays C_s symmetry, $^2A'$ electronic state and has a structure of a capped pentagonal bipyramid similar to **7n-1**, but with a Si atom capping on a Ti–Si–Si face. Structure **7a-2** is a bicapped triangular prism with two Si atoms capping on two Si–Si edges respectively. It is energetically 6.00 kcal/mol higher than the ground state **7a-1**. Structure **7a-3** is a bicapped square bipyramid and is less stable than **7a-1** by 13.48 kcal/mol. Similar to neutral **7n-3**, **7a-3** has two Si-capped Si–Si–Si faces. Isomer **7a-4** is a capped pentagonal bipyramid, more regular than neutral **7n-1**, being 14.49 kcal/mol above the ground state.

The lowest-energy state of cationic TiSi_7^+ has a distorted pentagonal bipyramid structure with one more Si atom capping on a Si–Si–Si face (**7c-1**), which is similar to the ground state of neutral TiSi_7 . Two tricapped trigonal bipyramid structures (**7c-2** and **7c-5**) can be viewed as adding a face-capping Si atom to structure **6c-4** of TiSi_6^+ . Isomers **7c-2** and **7c-5** are higher in energy than the ground state **7c-1** by 3.30 and 7.22 kcal/mol, respectively. Three bicapped square bipyramid structures (**7c-3**, **7c-6** and **7c-7**) are higher in energy than the ground state by 4.23, 9.91 and 10.74 kcal/mol, respectively. Structure **7c-4** is a distorted cube and 6.89 kcal/mol higher than the ground state.

$$n = 8$$

Structure **8n-1** is predicted to be the ground state of neutral TiSi_8 cluster, which can be seen as a Si atom face-capping on ground state structure of TiSi_7 (**7n-1**). The previous work of Guo et al. [29], got a distorted cube with the Ti atom on the surface site as ground state which we obtained as **8n-5**, 5.87 kcal/mol higher in energy than **8n-1**. Structures **8n-2** and **8n-3** are tricapped square bipyramid with different arrangement of capping Si atoms. They are 1.89 and 2.42 kcal/mol higher in energy than the ground **8n-1** state. Other low-lying isomers have bicapped pentagonal bipyramid geometries. Among them structures **8n-4**, **8n-6**, **8n-7**, **8n-8** and **8n-10** have the Ti atom on an apex and are 2.84–14.01 kcal/mol higher than the ground state, while structure **8n-9** has the Ti atom on an equatorial vertex and is 12.80 kcal/mol above the ground state.

Most of the low-lying structures we found for anionic TiSi_8^- can fall into two categories: tricapped square and bicapped pentagonal bipyramid with the Ti atom on an apex. The ground state (**8a-1**) is predicted to have a bicapped pentagonal bipyramid structure similar to neutral **8n-7** and its symmetry and electronic state are C_{2v} and 2B_1 , respectively. Other bicapped pentagonal bipyramid structures include **8a-2**, **8a-5**, **8a-6** and **8a-8**, differing in the placement of capping Si atoms. They are energetically above the ground state from 3.43 to 14.93 kcal/mol. Structure **8a-3**, **8a-4** and **8a-7** are tricapped square bipyramid, lying above the ground state **8a-1** by 7.37, 7.84 and 10.05 kcal/mol, respectively. Isomer **8a-9** can be described as two trigonal pyramids shared an apex of Ti atom and is 14.93 kcal/mol higher in energy than the ground state.

Almost all low-lying structures obtained for cationic TiSi_8^+ are bicapped pentagonal bipyramid. The ground state **8c-1** has the Ti atom located on an equatorial position. Its symmetry and electronic state are C_{2v} and 2A_1 , respectively. Other pentagonal bipyramid structures (**8c-2**, **8c-3**, **8c-5**, **8c-6** and **8c-7**) all have the Ti atom on an apex and are energetically above the ground state by 2.72–15.35 kcal/mol. Isomer **8c-4** is the only low-lying tricapped square bipyramid structure and is 5.99 kcal/mol above the ground state.

A comparison of the lowest-energy structures of $\text{TiSi}_n^-/\text{TiSi}_n^-/\text{TiSi}_n^+$ with those of $\text{Si}_{n+1}/\text{Si}_{n+1}^-/\text{Si}_{n+1}^+$, $\text{Si}_n/\text{Si}_n^-/\text{Si}_n^+$ [72], or $\text{TiSi}_{n-1}/\text{TiSi}_{n-1}^-/\text{TiSi}_{n-1}^+$

Summarily, triangular $\text{TiSi}_2/\text{TiSi}_2^-/\text{TiSi}_2^+$ are substitutive derivatives of $\text{Si}_3/\text{Si}_3^-/\text{Si}_3^+$ or adsorptive derivatives of a Ti atom to $\text{Si}_2/\text{Si}_2^-/\text{Si}_2^+$. Trigonal pyramidal TiSi_3 is an adsorptive derivative of a Ti atom to trigonal Si_3 , while rhombic $\text{TiSi}_3^-/\text{TiSi}_3^+$ are substitutive derivatives of rhombic $\text{Si}_4/\text{Si}_4^+$ or adsorptive derivatives of a Ti atom to trigonal $\text{Si}_3^-/\text{Si}_3^+$. Trigonal bipyramidal $\text{TiSi}_4/\text{TiSi}_4^-/\text{TiSi}_4^+$ keep the shapes of $\text{Si}_5/\text{Si}_5^-/\text{Si}_5^+$. The lowest-energy structures of $\text{TiSi}_5/\text{TiSi}_5^-/\text{TiSi}_5^+$ can be viewed as distorted substitutive derivative of $\text{Si}_6/\text{Si}_6^-/\text{Si}_6^+$. Capped square bipyramidal TiSi_6 is an adsorptive derivative of a Ti atom to square bipyramidal Si_6 , while pentagonal bipyramidal $\text{TiSi}_6^-/\text{TiSi}_6^+$ are substitutive derivative of $\text{Si}_7^-/\text{Si}_7^+$. Furthermore, all the lowest-energy structures of $\text{TiSi}_n/\text{TiSi}_n^-/\text{TiSi}_n^+$ can be derived from those of $\text{TiSi}_{n-1}/\text{TiSi}_{n-1}^-/\text{TiSi}_{n-1}^+$ by adsorbing a Si atom.

Energetic Properties

To compare the relative stability of clusters with different size, the average binding energy (E_b), fragmentation energy (E_f), and second-order energy difference (Δ_2E) were computed for all $\text{TiSi}_n/\text{TiSi}_n^-/\text{TiSi}_n^+$ clusters based on their ground states discussed above. The E_b , E_f and Δ_2E values were defined using the formulas followed:

$$\begin{aligned} E_b(\text{TiSi}_n) &= [E(\text{Ti}) + nE(\text{Si}) - E(\text{TiSi}_n)]/(n+1) \\ E_b(\text{TiSi}_n^-) &= [E(\text{Ti}) + (n-1)E(\text{Si}) + E(\text{Si}^-) - E(\text{TiSi}_n^-)]/(n+1) \\ E_b(\text{TiSi}_n^+) &= [E(\text{Ti}^+) + nE(\text{Si}) - E(\text{TiSi}_n^+)]/(n+1) \\ E_f(\text{TiSi}_n) &= E(\text{TiSi}_{n-1}) + E(\text{Si}) - E(\text{TiSi}_n) \\ E_f(\text{TiSi}_n^-) &= E(\text{TiSi}_{n-1}^-) + E(\text{Si}) - E(\text{TiSi}_n^-) \\ E_f(\text{TiSi}_n^+) &= E(\text{TiSi}_{n-1}^+) + E(\text{Si}) - E(\text{TiSi}_n^+) \\ \Delta_2E(\text{TiSi}_n) &= E(\text{TiSi}_{n+1}) + E(\text{TiSi}_{n-1}) - 2E(\text{TiSi}_n) \\ \Delta_2E(\text{TiSi}_n^-) &= E(\text{TiSi}_{n+1}^-) + E(\text{TiSi}_{n-1}^-) - 2E(\text{TiSi}_n^-) \\ \Delta_2E(\text{TiSi}_n^+) &= E(\text{TiSi}_{n+1}^+) + E(\text{TiSi}_{n-1}^+) - 2E(\text{TiSi}_n^+) \end{aligned}$$

where $E(M)$ represents the ground state energy of the M entity.

Average Binding Energies

The average binding energies (E_b) for the most stable isomers of the $\text{TiSi}_n/\text{TiSi}_n^-/\text{TiSi}_n^+$ clusters are shown in Fig. 3. The E_b values generally increase with increasing cluster size, therefore the clusters can continue to gain energy during the growth process. Comparing the three curves, the E_b values of neutral TiSi_n clusters are smaller than those of anionic TiSi_n^- clusters but larger than those of cationic TiSi_n^+ clusters, which may mean that the addition of an electron improves the stability of the TiSi_n clusters while the removal of an electron reduces it.

Fragmentation Energies

Figure 4 illustrates the fragmentation energies (E_f) for the most stable isomers of the $\text{TiSi}_n/\text{TiSi}_n^-/\text{TiSi}_n^+$ clusters as a function of cluster size, n . There are peaks at $n = 5$ and possibly also $n = 8$, except smaller $\text{TiSi}_2/\text{TiSi}_2^-/\text{TiSi}_2^+/\text{TiSi}_3^+$ clusters, and a trough at $n = 7$ for all neutral and charged Ti-doped silicon clusters, revealing that clusters at the size of $n = 5$ is more stable than those at $n = 4$ and 6, and clusters at the size of $n = 8$ is more stable than that at $n = 7$; meanwhile, clusters at the size of $n = 7$ is more active. Predictably, the $\text{TiSi}_5/\text{TiSi}_5^-/\text{TiSi}_5^+$ and $\text{TiSi}_8/\text{TiSi}_8^-/\text{TiSi}_8^+$ clusters may have high abundance in the mass spectrum.

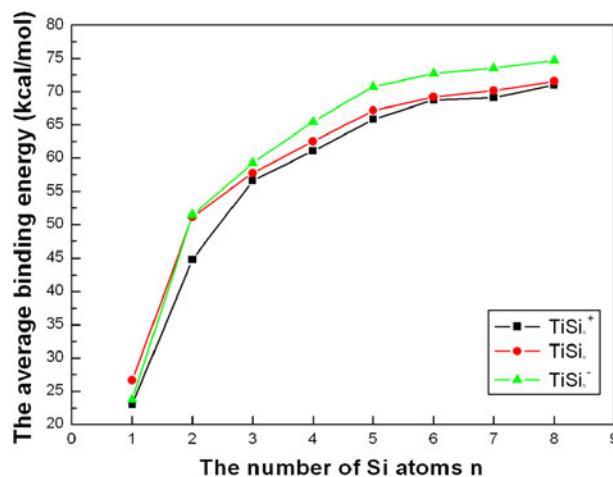


Fig. 3 Size dependence of the average binding energies for the most stable isomers of the $\text{TiSi}_n^-/\text{TiSi}_n^-/\text{TiSi}_n^+$ ($n = 1-8$) clusters

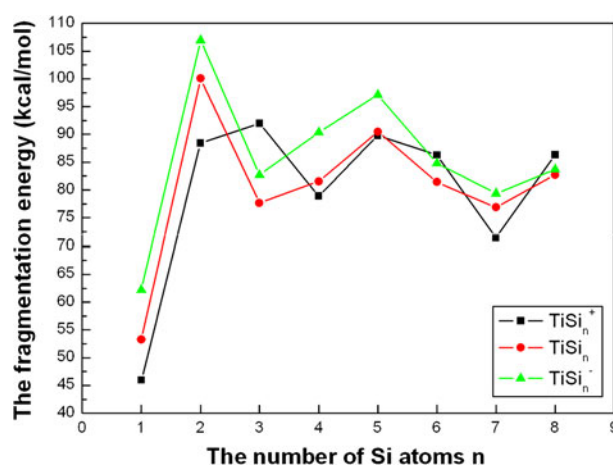


Fig. 4 Size dependence of the fragmentation energies for the most stable isomers of the $\text{TiSi}_n^-/\text{TiSi}_n^-/\text{TiSi}_n^+$ ($n = 1-8$) clusters

Second-Order Difference of Energies

The second-order difference of energies (Δ_2E) for the most stable isomers of the $\text{TiSi}_n^-/\text{TiSi}_n^-/\text{TiSi}_n^+$ clusters are provided in Fig. 5. The curves for neutral and anionic clusters have almost same trends, only different from each other at $n = 3$ and 4; they both have maximum at $n = 5$, except smaller $\text{TiSi}_2^-/\text{TiSi}_2^-$ clusters. For cationic clusters, the curve has a peak at $n = 6$ except smaller TiSi_3^+ , implying the corresponding TiSi_6^+ cluster is more stable than its neighboring clusters.

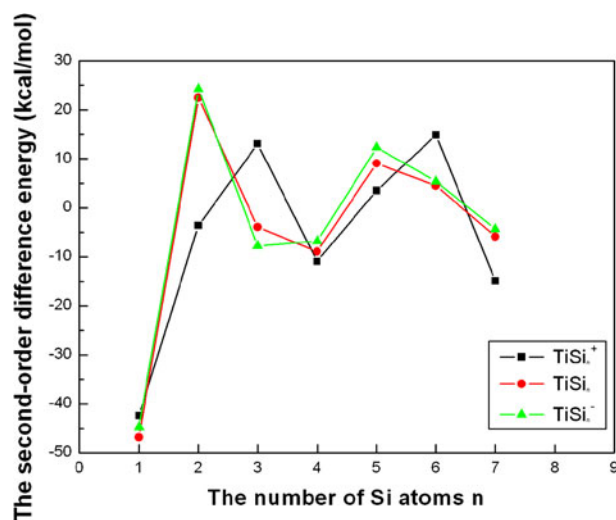


Fig. 5 Size dependence of the second-order difference of energies for the most stable isomers of the $\text{TiSi}_n/\text{TiSi}_n^-/\text{TiSi}_n^+$ ($n = 1-7$) clusters

HOMO–LUMO Gaps

The energy difference between the highest occupied and the lowest unoccupied molecular orbitals, the HOMO–LUMO gap, is a typical electronic property, which can help us understand the stability of clusters, i.e. the wider gap, the higher stability. Figure 6 gives the HOMO–LUMO gaps for the most stable structures of neutral and charged Ti-doped silicon clusters at each size. The HOMO–LUMO gaps

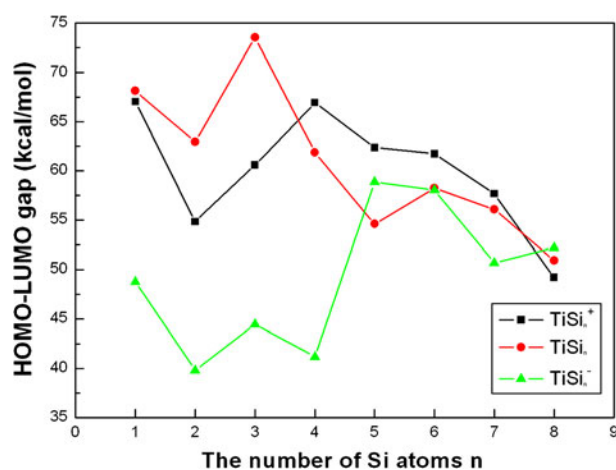


Fig. 6 Size dependence of the HOMO–LUMO gaps for the most stable isomers of the $\text{TiSi}_n/\text{TiSi}_n^-/\text{TiSi}_n^+$ ($n = 1-8$) clusters

are larger for neutral TiSi_3 and TiSi_6 , plus anionic TiSi_5^- and cationic TiSi_4^+ , indicating that these clusters have weaker chemical reactivity than their neighbors.

Ionization Potential and Electron Affinity

Other important properties that reflect the stability of clusters are their ionization potentials (IPs) and electron affinities (EAs). Comparing the total energies of TiSi_n , TiSi_n^+ and TiSi_n^- , we get the IP and EA values of the TiSi_n clusters. Three forms of the IP are reported herein, evaluated as the difference of total energies in the following manner:

the adiabatic IP are determined by

$$\text{AIP}(\text{TiSi}_n) = E(\text{optimized TiSi}_n^+) - E(\text{optimized TiSi}_n),$$

the vertical IP by

$$\text{VIP}(\text{TiSi}_n) = E(\text{TiSi}_n^+ \text{ at optimized neutral geometry}) - E(\text{optimized TiSi}_n),$$

and the vertical attachment energy of the cation by

$$\text{VAE}(\text{TiSi}_n) = E(\text{optimized TiSi}_n^+) - E(\text{TiSi}_n \text{ at optimized cationic geometry}).$$

Since the total energy of the optimized cation, $E(\text{optimized TiSi}_n^+)$, is lower than the total energy of the cation at the optimized neutral geometry, $E(\text{TiSi}_n^+ \text{ at optimized neutral geometry})$, and the total energy of the optimized neutral molecule, $E(\text{optimized TiSi}_n)$, is lower than the total energy of the neutral molecule at the optimized cation geometry, $E(\text{TiSi}_n \text{ at optimized cation geometry})$, three forms of IP should have an order of $\text{VAE} < \text{AIP} < \text{VIP}$. Thus, the VAE gives the lower bound while the VIP gives the upper bound, as shown in Fig. 7. The difference among AIP, VIP and VAE for the same cluster size is small when $n = 1, 2, 4, 5$ and 7 , since the geometries of these cationic clusters do not differ greatly from corresponding neutral clusters. On the other hand, when $n = 3, 6$ and 8 , the difference among AIP, VIP and VAE for the same cluster size is great, because the geometries of these cations differ significantly from the corresponding neutral clusters. The AIP values of TiSi_3 and TiSi_6 are smaller, suggesting that these clusters are more easily ionized than the others.

Similarly, there are also three forms of electron affinity, according to the following energy differences:

The adiabatic electron affinity are determined by

$$\text{AEA}(\text{TiSi}_n) = E(\text{optimized TiSi}_n) - E(\text{optimized TiSi}_n^-),$$

the vertical electron affinity by

$$\text{VEA}(\text{TiSi}_n) = E(\text{optimized TiSi}_n) - E(\text{TiSi}_n^- \text{ at optimized neutral geometry}),$$

and the vertical detachment energy of the anion by

$$\text{VDE}(\text{TiSi}_n) = E(\text{TiSi}_n \text{ at optimized anionic geometry}) - E(\text{optimized TiSi}_n^-),$$

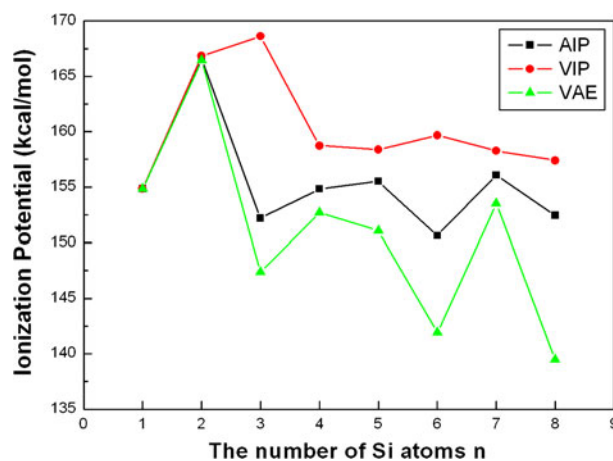


Fig. 7 Size dependence of the IPs for the most stable isomers of the TiSi_n ($n = 1\text{--}8$) clusters

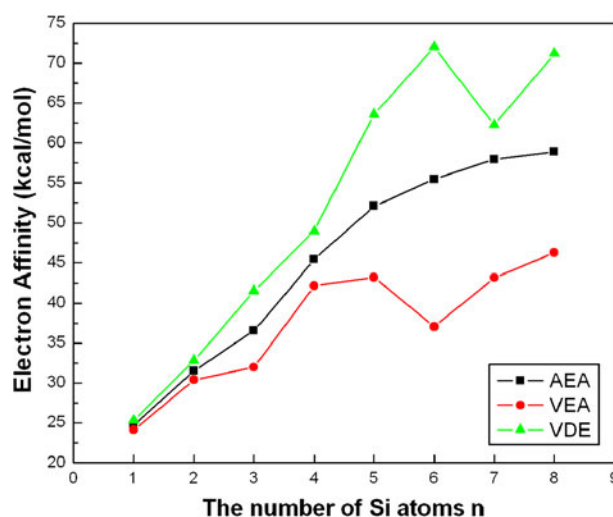


Fig. 8 Size dependence of the electron affinities for the most stable isomers of the TiSi_n ($n = 1\text{--}8$) clusters

with an EA order of $\text{VEA} < \text{AEA} < \text{VDE}$, the VEA giving the lower bound and the VDE giving the upper bound. As presented in Fig. 8, the AEA, VEA and VDE have similar values when $n = 1\text{--}4$ due to the small geometrical changes between neutral TiSi_n and its TiSi_n^- anions. The large geometrical differences between the global minima for $n = 5\text{--}8$ clusters leads to their AEA, VEA and VDE values much different. It is easily seen in Fig. 8 that there is a tendency to higher EAs as n increases.

Conclusion

Using DFT method at the B3LYP/6-311+G* level, the low-energy structures of neutral and charged Ti-doped silicon clusters $\text{TiSi}_n/\text{TiSi}_n^-/\text{TiSi}_n^+$ ($n = 1-8$) are obtained by considering a large number of structural isomers and several spin configurations, indicating that all neutral TiSi_n clusters favor Si-capped TiSi_{n-1} structures. The global minima of TiSi_n ($n = 2-8$) have a Si-side-on TiSi adduct (isosceles triangle, **2n-1**), Si-face-capped TiSi_2 triangle (trigonal pyramid, **3n-1**), Si-face-capped TiSi_3 trigonal pyramid (trigonal bipyramid, **4n-1**), Si-face-capped TiSi_4 trigonal bipyramid (**5n-1**), Si-face-capped TiSi_5 square bipyramid (**6n-1**), Si-face-capped TiSi_6 pentagonal bipyramid (**7n-1**), and Si-face-capped TiSi_7 capped pentagonal bipyramid (**8n-1**) structure, respectively. The ground state structures obtained for the TiSi_n clusters agree with those of Guo et al. [29] except for TiSi_3 and TiSi_8 .

Adding or removing an electron greatly changes some ground state structures. The most stable structures of ionic $\text{TiSi}_3^-/\text{TiSi}_3^+$, TiSi_5^- and $\text{TiSi}_6^-/\text{TiSi}_6^+$ are Ti-edge-capped Si_3 triangle (Ti-tipped rhombus, **3a-1** and **3c-1**), square bipyramid (**5a-1**) and pentagonal bipyramid (**6a-1** and **6c-1**), respectively, which are all significantly different from those of the corresponding neutral cluster structures. Although TiSi_7^- , $\text{TiSi}_8^-/\text{TiSi}_8^+$ have similar ground state structure, capped or bicapped pentagonal bipyramid, with the corresponding neutral TiSi_7 or TiSi_8 cluster, the position of their Ti atom or capping Si atom is clearly different. On the other hand, the stereochemistry structures of ionic $\text{TiSi}_2^-/\text{TiSi}_2^+$, $\text{TiSi}_4^-/\text{TiSi}_4^+$, TiSi_5^+ and TiSi_7^+ ground states are very similar to those of the corresponding neutral clusters, differing only in their bond lengths and angles. The geometrical differences or similarities mentioned above have been confirmed by their calculated IP and EA values.

The average binding energies reveal that all the $\text{TiSi}_n^-/\text{TiSi}_n/\text{TiSi}_n^+$ clusters can continue to gain energy as the size increasing. The fragmentation energies and second-order energy differences suggest that neutral TiSi_5 , anionic TiSi_5^- and cationic TiSi_6^+ are relatively stable.

Acknowledgments This research was supported by the 973 program (2009CB226109) in China, the Guangdong provincial natural science foundation (10151063101000041) and the postdoctoral science foundation (20110490903) of China.

References

1. O. Chesnovsky, S. H. Yang, C. L. Pettiette, M. J. Craycraft, Y. Liu, and R. E. Smalley (1987). *Chem. Phys. Lett.* **138**, 119.
2. C. C. Arnold, T. N. Kitsopoulos, and D. M. Neumark (1993). *J. Chem. Phys.* **99**, 766.
3. C. C. Arnold and D. M. Neumark (1994). *J. Chem. Phys.* **100**, 1797.
4. C. C. Arnold and D. M. Neumark (1993). *J. Chem. Phys.* **99**, 3353.
5. T. N. Kitsopoulos, C. J. Chick, A. Weaver, and D. M. Neumark (1990). *J. Chem. Phys.* **93**, 6108.
6. C. Xu, T. R. Taylor, G. R. Burton, and D. M. Neumark (1998). *J. Chem. Phys.* **108**, 1395.
7. K. Raghavachari and C. M. Rohlffing (1988). *Chem. Phys. Lett.* **143**, 428.
8. C. M. Rohlffing and K. Raghavachari (1990). *Chem. Phys. Lett.* **167**, 559.
9. K. Raghavachari and C. M. Rohlffing (1992). *Chem. Phys. Lett.* **198**, 521.

10. C. M. Rohlfing and K. Raghavachari (1992). *J. Chem. Phys.* **96**, 2114.
11. K. Raghavachari and C. M. Rohlfing (1988). *J. Chem. Phys.* **89**, 2219.
12. K. Raghavachari and C. M. Rohlfing (1991). *J. Chem. Phys.* **94**, 3670.
13. K. Raghavachari (1986). *J. Chem. Phys.* **84**, 5672.
14. K. Raghavachari (1985). *J. Chem. Phys.* **83**, 3520.
15. K. Raghavachari and V. Logovinsky (1985). *Phys. Rev. Lett.* **55**, 2853.
16. L. A. Curtiss, P. W. Deutsch, and K. Raghavachari (1992). *J. Chem. Phys.* **96**, 6868.
17. K. Raghavachari (1989). *Z. Phys. D* **12**, 61.
18. K. Raghavachari (1990). *Phase Transit.* **24–26**, 61.
19. R. Fournier, S. B. Sinnott, and A. E. DePristo (1992). *J. Chem. Phys.* **97**, 4149.
20. R. O. Jones (1999). *J. Chem. Phys.* **110**, 5189.
21. K.-M. Ho, A. A. Shvartsburg, B. Pan, Z.-Y. Lu, C.-Z. Wang, J. G. Wacker, J. Fye, and M. F. Jarrold (1998). *Nature* **392**, 582.
22. F. Hagelberg, J. Leszczynski, and V. Murashov (1998). *J. Mol. Struct. Theochem* **454**, 209.
23. I. Rata, A. A. Shvartsburg, M. Horoi, T. Frauenheim, K. W. Michael Siu, and K. A. Jackson (2000). *Phys. Rev. Lett.* **85**, 546.
24. S. M. Beck (1987). *J. Chem. Phys.* **87**, 4233.
25. S. M. Beck (1989). *J. Chem. Phys.* **90**, 6306.
26. H. Hiura, T. Miyazaki, and T. Kanayama (2001). *Phys. Rev. Lett.* **86**, 1733.
27. C. Y. Xiao, A. Abraham, R. Quinn, F. Hagelberg, and W. A. Lester Jr (2002). *J. Phys. Chem. A* **106**, 11380.
28. H. G. Xu, M. M. Wu, Z. G. Zhang, Q. Sun, and W. J. Zheng (2011). *Chin. Phys. B* **20**, (4), 043102.
29. L. J. Guo, X. Liu, G. F. Zhao, and Y. H. Luo (2007). *J. Chem. Phys.* **126**, 234704.
30. H. G. Xu, Z. G. Zhang, Y. Feng, J. Y. Yuan, Y. C. Zhao, and W. J. Zheng (2010). *Chem. Phys. Lett.* **487**, 204.
31. J. G. Han and F. Hagelberg (2001). *Chem. Phys.* **263**, 255.
32. H. Kawamura, V. Kumar, and Y. Kawazoe (2004). *Phys. Rev. B* **70**, 245433.
33. W. J. Zheng, J. M. Nilles, D. Radisic, and K. H. Bowen (2005). *J. Chem. Phys.* **122**, 071101.
34. J. R. Li, G. H. Wang, C. H. Yao, Y. W. Mu, J. G. Wan, and M. Han (2009). *J. Chem. Phys.* **130**, 164514.
35. L. Ma, J. J. Zhao, J. G. Wang, B. L. Wang, Q. L. Lu, and G. H. Wang (2006). *Phys. Rev. B* **73**, 125439.
36. S. N. Khanna, B. K. Rao, P. Jena, and S. K. Nayak (2006). *Chem. Phys. Lett.* **373**, 433.
37. J. G. Wang, J. J. Zhao, L. Ma, B. L. Wang, and G. H. Wang (2007). *Phys. Lett. A* **367**, 335.
38. Z. Y. Ren, F. Li, P. Guo, and J. G. Han (2005). *J. Mol. Struct. Theochem* **718**, 165.
39. J. R. Li, C. H. Yao, Y. W. Mu, J. G. Wan, and M. Han (2009). *J. Mol. Struct. Theochem* **916**, 139.
40. J. Wang, Q. M. Ma, Z. Xie, Y. Liu, and Y. C. Li (2007). *Phys. Rev. B* **76**, 035406.
41. C. Y. Xiao, F. Hagelberg, and W. A. Lester Jr (2002). *Phys. Rev. B* **66**, 075425.
42. Y. Z. Lan and Y. L. Feng (2009). *Phys. Rev. A* **79**, 033201.
43. A. P. Yang, Z. Y. Ren, P. Guo, and G. H. Wang (2008). *J. Mol. Struct. Theochem* **856**, 88.
44. J. Wang and J. G. Han (2005). *J. Chem. Phys.* **123**, 064306.
45. J. G. Han and F. Hagelberg (2001). *J. Mol. Struct. Theochem* **549**, 165.
46. F. C. Chuang, Y. Y. Hsieh, C. C. Hsu, and M. A. Albao (2007). *J. Chem. Phys.* **127**, 144313.
47. P. Guo, Z. Y. Ren, F. Wang, J. Bian, J. G. Han, and G. H. Wang (2004). *J. Chem. Phys.* **121**, 12265.
48. P. Guo, Z. Y. Ren, A. P. Yang, J. G. Han, J. Bian, and G. H. Wang (2006). *J. Phys. Chem. A* **110**, 7453.
49. J. G. Han, C. Y. Xiao, and F. Hagelberg (2002). *Struct. Chem.* **13**, 173.
50. J. G. Han, Z. Y. Ren, and B. Z. Lu (2004). *J. Phys. Chem. A* **108**, 5100.
51. J. G. Han (2003). *Chem. Phys.* **286**, 181.
52. J. Wang, Y. Liu, and Y. C. Li (2010). *Phys. Lett. A* **374**, 2736.
53. V. T. Ngan, P. Gruene, P. Claes, E. Janssens, A. Fielicke, M. T. Nguyen, and P. Lievens (2010). *J. Am. Chem. Soc.* **132**, 15589.
54. P. Claes, E. Janssens, V. T. Ngan, P. Gruene, J. T. Lyon, D. J. Harding, A. Fielicke, M. T. Nguyen, and P. Lievens (2011). *Phys. Rev. Lett.* **107**, 173401.
55. H.-K. Lin, Y.-F. Tzeng, C.-H. Wang, N.-H. Tai, I.-N. Lin, C.-Y. Lee, and H.-T. Chiu (2008). *Chem. Mater.* **20**, 2429.
56. E. Bucher, S. Schultz, M. C. Lux-Steiner, P. Munz, U. Gubler, and F. Greuter (1986). *Appl. Phys. A Mater. Sci. Process* **40**, 71.

57. S. P. Murarka and D. B. Fraser (1980). *J. Appl. Phys.* **51**, 350.
58. M. Ohara, K. Koyasu, A. Nakajima, and K. Kaya (2003). *Chem. Phys. Lett.* **371**, 490.
59. K. Koyasu, M. Akutsu, M. Mitsui, and A. Nakajima (2005). *J. Am. Chem. Soc.* **127**, 4998.
60. P. Sen and L. Mitas (2003). *Phys. Rev. B* **68**, 155404.
61. H. Kawamura, V. Kumar, and Y. Kawazoe (2004). *Phys. Rev. B* **70**, 193402.
62. H. Kawamura, V. Kumar, and Y. Kawazoe (2005). *Phys. Rev. B* **71**, 075423.
63. C. L. Reis and J. M. Pacheco (2010). *J. Phys.: Condens. Matter* **22**, 035501.
64. M. J. Frisch, G. W. Trucks, H. B. Schlegel, G. E. Scuseria, M. A. Robb, J. R. Cheeseman, J. A. Montgomery, Jr., T. Vreven, K. N. Kudin, J. C. Burant, J. M. Millam, S. S. Iyengar, J. Tomasi, V. Barone, B. Mennucci, M. Cossi, G. Scalmani, N. Rega, G. A. Petersson, H. Nakatsuji, M. Hada, M. Ehara, K. Toyota, R. Fukuda, J. Hasegawa, M. Ishida, T. Nakajima, Y. Honda, O. Kitao, H. Nakai, M. Klene, X. Li, J. E. Knox, H. P. Hratchian, J. B. Cross, V. Bakken, C. Adamo, J. Jaramillo, R. Gomperts, R. E. Stratmann, O. Yazyev, A. J. Austin, R. Cammi, C. Pomelli, J. W. Ochterski, P. Y. Ayala, K. Morokuma, G. A. Voth, P. Salvador, J. J. Dannenberg, V. G. Zakrzewski, S. Dapprich, A. D. Daniels, M. C. Strain, O. Farkas, D. K. Malick, A. D. Rabuck, K. Raghavachari, J. B. Foresman, J. V. Ortiz, Q. Cui, A. G. Baboul, S. Clifford, J. Cioslowski, B. B. Stefanov, G. Liu, A. Liashenko, P. Piskorz, I. Komaromi, R. L. Martin, D. J. Fox, T. Keith, M. A. Al-Laham, C. Y. Peng, A. Nanayakkara, M. Challacombe, P. M. W. Gill, B. Johnson, W. Chen, M. W. Wong, C. Gonzalez, and J. A. Pople, *Gaussian 03, Revision D. 01* (Gaussian, Inc., Wallingford CT, 2004).
65. A. D. Becke (1993). *J. Chem. Phys.* **98**, 5648.
66. C. Lee, W. T. Yang, and R. G. Parr (1988). *Phys. Rev. B* **37**, 785.
67. R. Krishnan, J. S. Binkley, R. Seeger, and J. A. Pople (1980). *J. Chem. Phys.* **72**, 650.
68. L. A. Curtiss, M. P. McGrath, J. P. Blaudeau, N. E. Davis, R. C. Binning Jr, and L. Radom (1995). *J. Chem. Phys.* **103**, 6104.
69. A. J. H. Wachters (1970). *J. Chem. Phys.* **52**, 1033.
70. P. J. Hay (1977). *J. Chem. Phys.* **66**, 4377.
71. K. Raghavachari and G. W. Trucks (1989). *J. Chem. Phys.* **91**, 1062.
72. A. A. Shvartsburg, B. Liu, M. F. Jarrold, and K. M. Ho (2000). *J. Chem. Phys.* **112**, 4517.